
How Initial Connectivity Shapes Biologically Plausible Learning in Recurrent Neural Networks

Weixuan Liu^{1,*}, Xinyue Zhang^{2,*}, and Yuhan Helena Liu^{3,+}

¹University of Washington, Seattle, WA, USA

²Columbia University, New York, NY, USA

³Princeton University, Princeton, NJ, USA

*Joint first authors, listed in random order

+Correspondence: hl7582@princeton.edu

Abstract

The impact of initial connectivity on learning has been extensively studied in the context of backpropagation-based gradient descent, but it remains largely underexplored in biologically plausible learning settings. Focusing on recurrent neural networks (RNNs), we found that the initial weight magnitude significantly influences the learning performance of biologically plausible learning rules in a similar manner to its previously observed effect on training via backpropagation through time (BPTT). By examining the maximum Lyapunov exponent before and after training, we uncovered the greater demands that certain initialization schemes place on training to achieve desired information propagation properties. Consequently, we extended the recently proposed gradient flossing method, which regularizes the Lyapunov exponents, to biologically plausible learning and observed an improvement in learning performance. To our knowledge, we are the first to examine the impact of initialization on biologically plausible learning rules for RNNs and to subsequently propose a biologically plausible remedy. Such an investigation could lead to predictions about the influence of initial connectivity on learning dynamics and performance, as well as guide neuromorphic design.

1 Introduction

A central question in computational neuroscience is how initial connectivity influences the dynamics of learning. While the magnitude of initial weights is known to influence these dynamics in backpropagation-based gradient descent learning [1, 2, 3, 4, 5, 6, 7], the neural implementation challenges of backpropagation [8, 9, 10] raise important questions about how such influence extend to biologically plausible learning [8, 11, 12, 13, 14, 15, 16, 17, 18, 19, 20, 21, 22, 23, 24, 25, 26, 27]. This inquiry is especially relevant for recurrent neural networks (RNNs), which are widely employed in modeling neural circuits [28, 29, 30].

In light of this, we ask: How does the initialization of weights, particularly their magnitude, affect the performance of biologically plausible learning in RNNs? We evaluate performance primarily through learning curves, measured by the reduction in loss over training. Our focus is on biologically plausible learning rules that approximate gradients by truncating non-biological terms, specifically the two equivalent rules of e-prop and random feedback local online (RFLO) learning, which have shown efficacy and adaptability in solving complex tasks [20, 21, 31]. Our contributions are as follows:

- We demonstrate that, much like in BPTT, the initial weight magnitude in e-prop significantly affects learning performance (Figure 1).

- To explain this result, we identified that the maximum Lyapunov exponent — crucial for the stability of information propagation — undergoes the most significant changes with small initial weight magnitudes, suggesting greater demands are placed on training (Figure 3).
- Consequently, we extended the recently proposed gradient flossing method [32] — designed to stabilize Lyapunov exponents — to the context of biologically plausible learning. This approach led to a significant improvement in performance (Figure 4), particularly when the initial weight magnitude was suboptimal, which might occur due to pathological conditions.

2 Results

2.1 Network and training setup

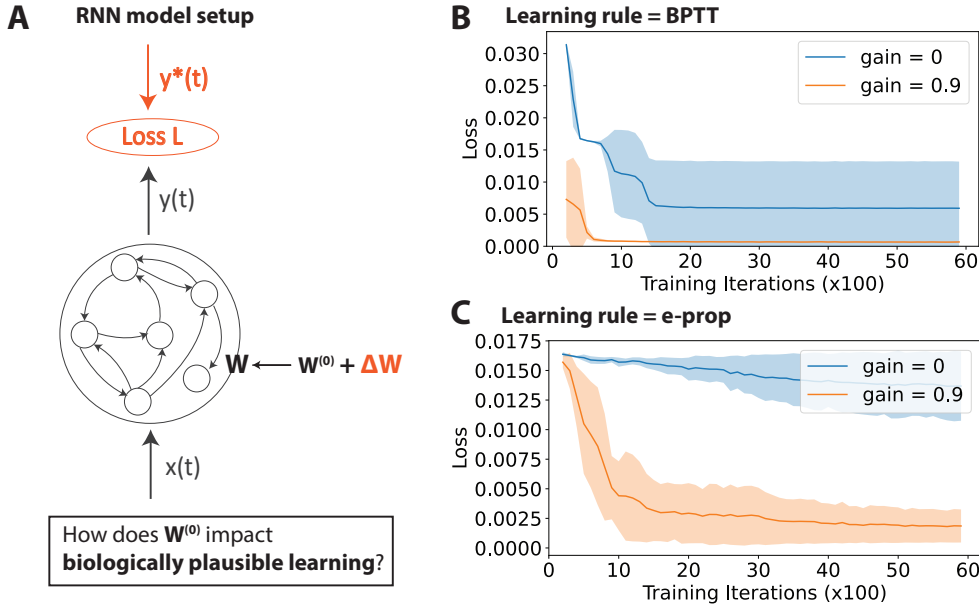


Figure 1: Influence of weight initialization on biologically plausible learning. A) Recurrent neural network (RNN) learning setup. B) Loss curves throughout training for different initial gains using the standard back-propagation through time (BPTT) algorithm. Here, gain reflects the initial weight magnitude: recurrent weights are initialized as $W_{h,ij}^{(0)} \sim \mathcal{N}(0, \text{gain}^2/N)$. C) Loss curve throughout training for different initial gains using e-prop, a biologically plausible learning rule for RNNs. Note: the plots in B) and C) begin after 200 training iterations to provide a more focused view of the results. This figure illustrates the Romo task but similar trends are observed for the 2AF and DMS tasks (Figure 2). Learning curves for more intermediate gain values are examined in Appendix Figure 5. Solid lines/shaded regions: mean/standard deviation of loss curves across independent runs with different seeds.

We examine recurrent neural networks (RNNs) because they are commonly adopted for modeling neural circuits [33, 34]. Our RNN model (Figure 1A) comprises N_{in} input nodes, N hidden nodes, and N_{out} output nodes. The hidden state at time t , denoted as $h_t \in \mathbb{R}^N$, is updated according to the following equation:

$$h_{t+1} = \alpha h_t + (1 - \alpha)(W_h f(h_t) + W_x x_t), \quad (1)$$

where the leak factor $\alpha = 1 - \frac{dt}{\tau} \in \mathbb{R}$ is determined by the simulation time step dt and the membrane time constant τ . The function $f(\cdot) : \mathbb{R}^N \rightarrow \mathbb{R}^N$ is the *ReLU* activation function; $W_h \in \mathbb{R}^{N \times N}$ and $W_x \in \mathbb{R}^{N \times N_{in}}$ represent the recurrent and input weight matrices, respectively; and $x_t \in \mathbb{R}^{N_{in}}$ is the input at time t . The output, $\hat{y}_t \in \mathbb{R}^{N_{out}}$, is derived as a linear combination of the hidden state activation, $f(h_t)$, using the readout weights $w \in \mathbb{R}^{N_{out} \times N}$.

The goal is to minimize the scalar loss $L \in \mathbb{R}$. For loss minimization, we explored several learning rules, including BPTT, which calculates the exact gradient, $\nabla_W L(W_h) \in \mathbb{R}^{N \times (N_{in} + N + N_{out})}$, as well as biologically plausible learning rules that utilize approximate gradients, $\widehat{\nabla}_W L(W) \in$

$\mathbb{R}^{N \times (N_{in} + N + N_{out})}$:

$$\Delta W = -\eta \nabla_W L(W), \quad (2)$$

$$\widehat{\Delta W} = -\eta \widehat{\nabla}_W L(W), \quad (3)$$

where $W = [W_h \ W_x \ w^T] \in \mathbb{R}^{N \times (N_{in} + N + N_{out})}$ represents all the trainable parameters, and $\eta \in \mathbb{R}$ is the learning rate.

In the realm of biologically plausible learning rules for RNNs, we focused primarily on e-prop [21] and RFLO [20], which rely on gradient truncation. Since both are equivalent in our setting, we present only the results for e-prop. A significant challenge with the neural implementation of BPTT arises from its weight updates, which require precise gradients of the loss with respect to the weights. This process demands that every synapse receive activity signals from the entire recurrent network [24], a mechanism that raises serious questions about its validity for modeling neural circuit learning. In contrast, e-prop and RFLO truncate this exact gradient, ensuring that the remaining terms can be associated with known biological processes; specifically, the weight update depends on the pre- and postsynaptic activities along with a third factor that guides the weight update. Although other biologically plausible learning rules exist, we concentrated on e-prop and RFLO due to their versatility and being the focus of recent studies examining RNN learning rules [25, 35]. For example, rules like equilibrium propagation depend on the equilibrium condition [11, 19].

We simulated different neuroscience tasks. In the main text, we displayed results for the Romo task [36], following the implementation in [3], but also showed the trend applies to other tasks — including perceptual decision-making (2AF) and the delayed-match-to-sample (DMS) tasks — implemented using Neurogym [29] (Figure 2). More training details can be found in Appendix A.

2.2 Simulation results

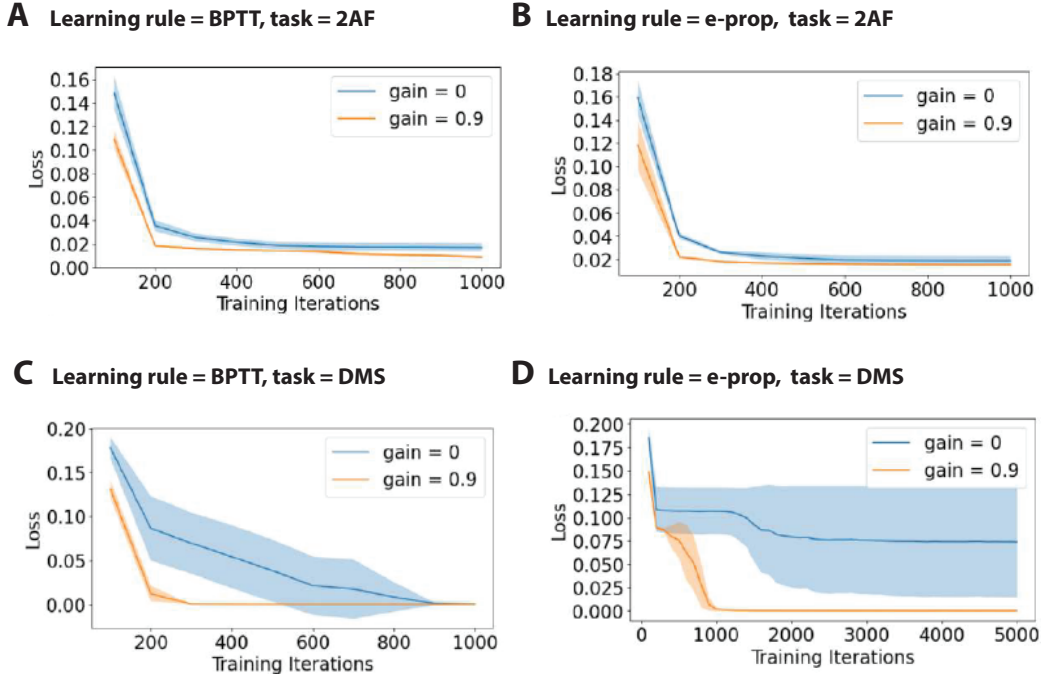


Figure 2: Similar trends as Figure 1 observed for the 2AF and DMS tasks. A) Learning curve for the 2AF task across different initial gains using backpropagation through time (BPTT). B) Similar to A) but for e-prop. C) Similar to A) but for the DMS task. D) Similar to B) but for the DMS task. Plotting convention follows that of Figure 1.

We examined the effects of different initial weight magnitudes, which have been shown to significantly influence the learning trajectory and final solution in BPTT [3]. Figure 1 demonstrates that the performance gap, as indicated by the learning curve, is substantial across different initialization magnitudes for both BPTT and e-prop. Additional intermediate magnitudes are explored in Appendix

Figure 5, where notable gap is observed for certain initial weight magnitudes. Similar trends are evident when the experiments are repeated across other tasks, specifically the 2AF and DMS tasks implemented using Neurogym (Figure 2). These results underscore the critical role of weight initialization in biologically plausible learning.

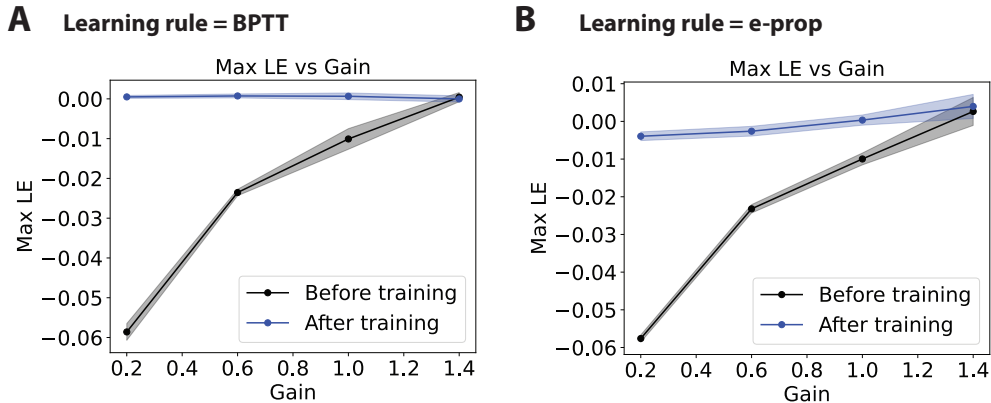


Figure 3: The maximum Lyapunov exponent (Max LE) computed before and after training across various weight initialization gains for training via A) BPTT and B) e-prop. Gain is defined similarly as in Figure 1. Certain initial weight magnitudes result in more significant changes in the Max LE. Solid lines/shaded regions: mean/standard deviation of Max LE across independent runs with different seeds.

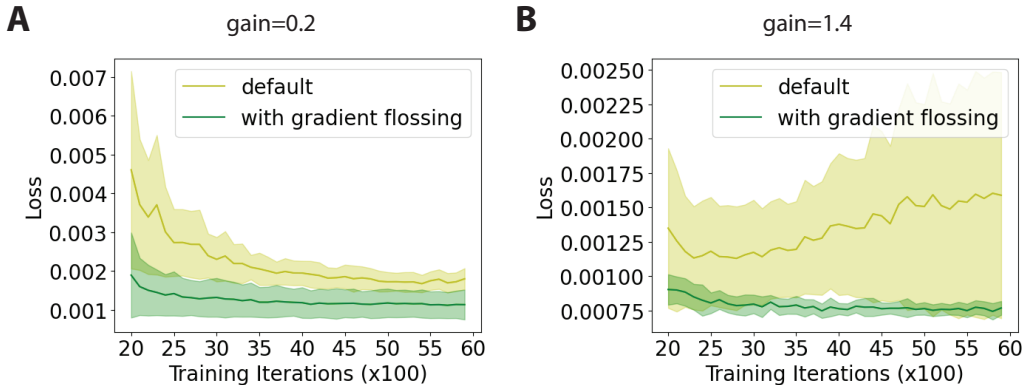


Figure 4: Initialization via pretraining with gradient flossing improves e-prop learning performance, particularly for suboptimal initialization gains. Note: The plot begins after 2000 iterations to provide a more focused view of the results.

Next, we investigate why initialization has such a profound effect on learning performance in biologically plausible learning. We turn to Lyapunov exponents, which can reflect the ability of RNNs to propagate information [37]. Lyapunov exponents help in studying the dynamical properties of RNNs, as they measure the system’s sensitivity to initial conditions and quantify the rates of divergence or convergence of trajectories in the system’s state space [38]. We computed the Lyapunov exponent using the method described in [37] for networks before and after training. The analysis was done for the Romo task but similar trends were observed for other tasks as well. As expected, the trained networks exhibit a maximum Lyapunov exponent around 0, so that the signals neither explode nor vanish. However, before training, networks initialized with smaller weight gains had Lyapunov exponents further from 0, indicating that more changes are required via training, thus making the process more challenging for such initializations (Figure 3).

To address this, we applied the recently proposed gradient flossing method [32], which adjusts Lyapunov exponents closer to 0 and has been shown to improve BPTT training performance. We adapted this method for biologically plausible learning by pretraining the network with 100 iterations using the "flossing loss" while ensuring the weight updates use local information only (see Appendix), a loss function defined based on the squared sum of the Lyapunov exponent. Our results show that

this approach of gradient flossing also enhances performance in this context of biologically plausible learning, particularly when the initial weight gain is suboptimal (Figure 4), which might happen due to pathology.

3 Discussion

The results of this study underscore the role of initial weight magnitude in shaping the learning dynamics of recurrent neural networks (RNNs), specifically within the context of biologically plausible learning rules. While the influence of initial connectivity on learning has been extensively explored in the realm of backpropagation-based learning, our work is novel because it extends this inquiry to biologically plausible settings. Our findings demonstrate that, similar to backpropagation through time (BPTT), the choice of initial weight magnitude in e-prop — a biologically plausible learning rule — has a profound impact on learning performance. Notably, we observed that smaller initial gains, which theoretically reduce gradient truncation errors, can paradoxically hinder learning. This counterintuitive result is explained by our analysis of the Lyapunov exponent, which is crucial for the stability and information propagation within the network. We found that smaller initial gains resulted in larger deviations of the Lyapunov exponent from zero before training, indicating a greater challenge in achieving stable dynamical properties through training. To address this challenge, we brought the gradient flossing method into the biologically plausible learning framework, leading to performance improvement for suboptimal initial weight magnitudes. Overall, these findings could lead to predictions on how different initial connectivity could influence learning in neural circuits. Additionally, these findings have practical implications for the design of neuromorphic chips, where optimizing initial weight configurations could enhance the efficiency and effectiveness of energy-efficient biologically plausible learning algorithms.

Extending our approach to study the interaction between initialization and biologically plausible learning rules across a broader spectrum of learning rules, architectures, and tasks is a crucial direction for future research. In this study, we focused on examining existing biologically plausible RNN learning rules [20, 21, 22], adopting a level of biological realism similar to that in those studies. We leave the exploration of more biologically realistic architectures to future work. Additionally, our primary emphasis was on truncation-based learning rules in RNNs, selected for their efficacy in task learning, versatility in settings (for instance, they do not rely on the equilibrium assumption [11, 19]), and being the focus of learning rule analysis in recent studies [25, 35]. An important future direction would involve exploring a wider range of learning rules, including reinforcement learning [39], beyond the supervised learning setup currently examined. Moreover, while we concentrated on the magnitude of initial connectivity since it was shown to play a significant role in influencing the learning dynamics of BPTT-based training [3], other attributes of initialization may also play a significant role [40]. We primarily assessed the impact in terms of task accuracy, but other aspects, such as the rich/lazy learning regimes and the subsequent generalization properties, remain to be examined [2, 41]. Overall, the space of interaction between initialization and biologically plausible learning dynamics is vast, integrating numerous factors, and our work is a stepping stone toward piecing together this complex area.

References

- [1] Timo Flesch, Keno Juechems, Tsvetomira Dumbalska, Andrew Saxe, and Christopher Summerfield. Rich and lazy learning of task representations in brains and neural networks. *BioRxiv*, pages 2021–04, 2021.
- [2] Lenaïc Chizat, Edouard Oyallon, and Francis Bach. On lazy training in differentiable programming. *Advances in neural information processing systems*, 32, 2019.
- [3] Friedrich Schuessler, Francesca Mastrogiuseppe, Alexis Dubreuil, Srdjan Ostojic, and Omri Barak. The interplay between randomness and structure during learning in rnns. *Advances in neural information processing systems*, 33:13352–13362, 2020.
- [4] Lukas Braun, Clémentine Dominé, James Fitzgerald, and Andrew Saxe. Exact learning dynamics of deep linear networks with prior knowledge. *Advances in Neural Information Processing Systems*, 35:6615–6629, 2022.

- [5] Blake Woodworth, Suriya Gunasekar, Jason D Lee, Edward Moroshko, Pedro Savarese, Itay Golan, Daniel Soudry, and Nathan Srebro. Kernel and rich regimes in overparametrized models. In *Conference on Learning Theory*, pages 3635–3673. PMLR, 2020.
- [6] Jonas Paccolat, Leonardo Petrini, Mario Geiger, Kevin Tyloo, and Matthieu Wyart. Geometric compression of invariant manifolds in neural networks. *Journal of Statistical Mechanics: Theory and Experiment*, 2021(4):044001, 2021.
- [7] Friedrich Schuessler, Francesca Mastrogiuseppe, Srdjan Ostojic, and Omri Barak. Aligned and oblique dynamics in recurrent neural networks. *arXiv preprint arXiv:2307.07654*, 2023.
- [8] Timothy P Lillicrap, Adam Santoro, Luke Marris, Colin J Akerman, and Geoffrey Hinton. Backpropagation and the brain. *Nature Reviews Neuroscience*, 21(6):335–346, 2020.
- [9] Blake A Richards, Timothy P Lillicrap, Philippe Beaudoin, Yoshua Bengio, Rafal Bogacz, Amelia Christensen, Claudia Clopath, Rui Ponte Costa, Archy de Berker, Surya Ganguli, et al. A deep learning framework for neuroscience. *Nature neuroscience*, 22(11):1761–1770, 2019.
- [10] Timothy P Lillicrap and Adam Santoro. Backpropagation through time and the brain. *Current opinion in neurobiology*, 55:82–89, 2019.
- [11] Benjamin Scellier and Yoshua Bengio. Equilibrium propagation: Bridging the gap between energy-based models and backpropagation. *Frontiers in computational neuroscience*, 11:24, 2017.
- [12] Sigurd Diederich and Manfred Opper. Learning of correlated patterns in spin-glass networks by local learning rules. *Physical review letters*, 58(9):949, 1987.
- [13] Geoffrey Hinton. The forward-forward algorithm: Some preliminary investigations. *arXiv preprint arXiv:2212.13345*, 2022.
- [14] Axel Laborieux and Friedemann Zenke. Holomorphic equilibrium propagation computes exact gradients through finite size oscillations. *arXiv preprint arXiv:2209.00530*, 2022.
- [15] Will Greedy, Heng Wei Zhu, Joseph Pemberton, Jack Mellor, and Rui Ponte Costa. Single-phase deep learning in cortico-cortical networks. *Advances in Neural Information Processing Systems*, 35:24213–24225, 2022.
- [16] João Sacramento, Rui Ponte Costa, Yoshua Bengio, and Walter Senn. Dendritic cortical microcircuits approximate the backpropagation algorithm. *arXiv preprint arXiv:1810.11393*, 2018.
- [17] Alexandre Payeur, Jordan Guerguiev, Friedemann Zenke, Blake A Richards, and Richard Naud. Burst-dependent synaptic plasticity can coordinate learning in hierarchical circuits. *Nature neuroscience*, pages 1–10, 2021.
- [18] Pieter R Roelfsema and Anthony Holtmaat. Control of synaptic plasticity in deep cortical networks. *Nature Reviews Neuroscience*, 19(3):166–180, 2018.
- [19] Alexander Meulemans, Nicolas Zucchet, Seijin Kobayashi, Johannes Von Oswald, and João Sacramento. The least-control principle for local learning at equilibrium. *Advances in Neural Information Processing Systems*, 35:33603–33617, 2022.
- [20] James M Murray. Local online learning in recurrent networks with random feedback. *Elife*, 8:e43299, 2019.
- [21] Guillaume Bellec, Franz Scherr, Anand Subramoney, Elias Hajek, Darjan Salaj, Robert Legenstein, and Wolfgang Maass. A solution to the learning dilemma for recurrent networks of spiking neurons. *Nature communications*, 11(1):3625, 2020.
- [22] Yuhan Helena Liu, Stephen Smith, Stefan Mihalas, Eric Shea-Brown, and Uygur Sümbül. Cell-type-specific neuromodulation guides synaptic credit assignment in a spiking neural network. *Proceedings of the National Academy of Sciences*, 118(51):e2111821118, 2021.
- [23] Yuhan Helena Liu, Stephen Smith, Stefan Mihalas, Eric Shea-Brown, and Uygur Sümbül. Biologically-plausible backpropagation through arbitrary timespans via local neuromodulators. *arXiv preprint arXiv:2206.01338*, 2022.
- [24] Owen Marschall, Kyunghyun Cho, and Cristina Savin. A unified framework of online learning algorithms for training recurrent neural networks. *The Journal of Machine Learning Research*, 21(1):5320–5353, 2020.

- [25] Yuhan Helena Liu, Arna Ghosh, Blake Richards, Eric Shea-Brown, and Guillaume Lajoie. Beyond accuracy: generalization properties of bio-plausible temporal credit assignment rules. *Advances in Neural Information Processing Systems*, 35:23077–23097, 2022.
- [26] Arna Ghosh, Yuhan Helena Liu, Guillaume Lajoie, Konrad Kording, and Blake Aaron Richards. How gradient estimator variance and bias impact learning in neural networks. In *The Eleventh International Conference on Learning Representations*, 2023.
- [27] Blake Bordelon and Cengiz Pehlevan. The influence of learning rule on representation dynamics in wide neural networks. *arXiv preprint arXiv:2210.02157*, 2022.
- [28] Guangyu Robert Yang and Xiao-Jing Wang. Artificial neural networks for neuroscientists: a primer. *Neuron*, 107(6):1048–1070, 2020.
- [29] Manuel Molano-Mazon, Joao Barbosa, Jordi Pastor-Ciurana, Marta Fradera, Ru-Yuan Zhang, Jeremy Forest, Jorge del Pozo Lerida, Li Ji-An, Christopher J Cueva, Jaime de la Rocha, et al. Neurogym: An open resource for developing and sharing neuroscience tasks. 2022.
- [30] Saurabh Vyas, Matthew D Golub, David Sussillo, and Krishna V Shenoy. Computation through neural population dynamics. *Annual Review of Neuroscience*, 43:249–275, 2020.
- [31] Roy Henha Eyono, Ellen Boven, Arna Ghosh, Joseph Pemberton, Franz Scherr, Claudia Clopath, Rui Ponte Costa, Wolfgang Maass, Blake A Richards, Cristina Savin, et al. Current state and future directions for learning in biological recurrent neural networks: A perspective piece. *Neurons, Behavior, Data analysis, and Theory*, 1, 2022.
- [32] Rainer Engelken. Gradient flossing: Improving gradient descent through dynamic control of jacobians. *Advances in Neural Information Processing Systems*, 36, 2024.
- [33] Omri Barak. Recurrent neural networks as versatile tools of neuroscience research. *Current opinion in neurobiology*, 46:1–6, 2017.
- [34] H Francis Song, Guangyu R Yang, and Xiao-Jing Wang. Training excitatory-inhibitory recurrent neural networks for cognitive tasks: a simple and flexible framework. *PLoS computational biology*, 12(2):e1004792, 2016.
- [35] Jacob Portes, Christian Schmid, and James M Murray. Distinguishing learning rules with brain machine interfaces. *Advances in neural information processing systems*, 35:25937–25950, 2022.
- [36] Ranulfo Romo, Carlos D Brody, Adrián Hernández, and Luis Lemus. Neuronal correlates of parametric working memory in the prefrontal cortex. *Nature*, 399(6735):470–473, 1999.
- [37] Ryan Vogt, Maximilian Puelma Touzel, Eli Shlizerman, and Guillaume Lajoie. On lyapunov exponents for rnns: Understanding information propagation using dynamical systems tools. *Frontiers in Applied Mathematics and Statistics*, 8:818799, 2022.
- [38] Manuel Casado, Juan Cantero-Águila, Ángel R. Sánchez, David Perales, Roberto Colom, and Javier Navarrete. Lyapunov exponents from time series. *Frontiers in Applied Mathematics and Statistics*, 8:818799, 2022.
- [39] Richard S Sutton. Reinforcement learning: an introduction. *A Bradford Book*, 2018.
- [40] Yuhan Helena Liu, Aristide Baratin, Jonathan Cornford, Stefan Mihalas, Eric Shea-Brown, and Guillaume Lajoie. How connectivity structure shapes rich and lazy learning in neural circuits. *ArXiv*, 2023.
- [41] Arthur Jacot, Franck Gabriel, and Clément Hongler. Neural tangent kernel: Convergence and generalization in neural networks. *Advances in neural information processing systems*, 31, 2018.

A Appendix / supplemental material

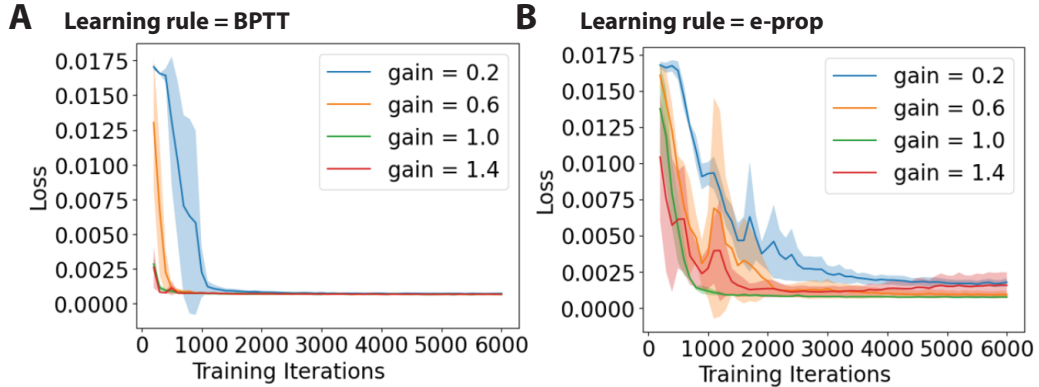


Figure 5: Figure 1 repeated for more intermediate gain values for A) BPTT and B) e-prop. Noticeable gap in the learning curve is observed between $gain = 0.2$ with the others before convergence, even with hyperparameter tuning. Plotting convention follows that of Figure 1.

Our RNN training was conducted using PyTorch using the Adam optimizer and built on the code in [28] (see the notebook *RNN + DynamicalSystemAnalysis.ipynb*). For the 2AF and DMS tasks, we used the default Neurogym settings, while for the Romo task, we followed the implementation from [3]. E-prop was implemented in PyTorch using `hidden.detach()`, where `hidden` is the hidden state tensor, to prevent gradient propagation across the hidden states, thereby effectively truncating the nonlocal gradient terms; this was also applied when pretraining via gradient flossing, ensuring the weight update uses location information only. Our performance evaluation utilized the learning curve, which tracks the reduction in the loss over training iterations. To give each initialization scheme a fair chance at success, we used the optimal learning rate for each initialization scheme selected from a grid of $[1e-4, 3e-4, 1e-3, 3e-3]$. By default, we used 64 hidden neurons and a batch size of 32, but similar trends were observed when doubling these. Each training iteration was replicated over five independent runs. All simulations were executed using Google Colab (the free version) with each run taking under 5 minutes to complete. We currently focus on recurrent weight initialization, employing standard random initialization for both the input and readout weights (initialized as in [28]).